EXTENDED DOMAIN FWI VIA TIME WARPING

G. Huang[1], J. Ramos-Martínez[1], Y. Yang[1], R. Djebbi[1], N. Chemingui[1]

[1] Petroleum Geo-Services

Summary

Overcoming cycle-skipping in Full Waveform Inversion (FWI) is a significant step toward enabling automation in velocity model building. This reduces the demand of acquiring very low frequency data and/or starting the inversion procedure from kinematically accurate models. We present a new FWI method that uses time-warping as the extension domain to overcome cycle-skipping. The warping function dynamically transports the recorded field data to the modeled data and is imposed to represent the actual physical time. Thus, the derived objective function allows the inversion of the two parameters involved, model and time-warping extension, in a single optimization problem, whose solution is provided by the Alternate Direction Method (ADM). The novel FWI objective function enables automatic transition from a pure time-shift problem to a conventional least-squares one. We successfully apply the new FWI method to both synthetic and field data sets to demonstrate its effectiveness starting from inaccurate initial models. Results show the benefits of the new FWI approach in reducing the turnaround time for building high-resolution models from very simple initial velocity models.

Extended domain FWI via time warping

Introduction

Conventional FWI is a nonlinear optimization problem that matches modeled data to recorded field data (Tarantola, 1984) in the least squares sense. The nonconvexity of the least-squares objective function needs the lowest possible frequencies or a kinematically accurate initial model, otherwise the conventional approach may be trapped in local minima caused by cycle-skipping (Virieux and Operto, 2009).

In the recent years, diverse methods have been proposed to mitigate the cycle-skipping problem and consequently reduce the turnaround time of multistage strategies. This includes time-lag based objective functions (e.g., Luo and Schuster, 1991; Ma and Hale, 2013), inversion with intermediate data sets (Wang et al., 2016; Yao et al., 2019) and extended domain waveform algorithms (Symes, 2008). For the extended FWI approaches, the domain of extension can be adopted either in the model space, like the time-lag extended reflectivity model (Biondi and Almomin, 2013), or in the data domain such as source extension (Huang et al., 2017) and receiver extension (Metivier et al., 2020). Data domain extensions are preferable because they avoid increasing the computational cost and the additional modeling steps required for the model extension-based methods.

We introduce a novel FWI method using the time-warping extension that minimizes the data fitting between the modeled and the warped field data by progressively updating the time-warping extension to represent the actual physical time. We formulate a new objective function in which the velocity model and time-warping extension are solved by the Alternate Direction Method (ADM) in a single non-linear optimization. The inner problem for the time-warping extension can be solved using dynamic programming similar to classic DTW (Sakoe and Chiba, 1978), but with an augmented cost function. This makes our method different than the existing DTW algorithms (e.g., Hale, 2013). The outer problem consists of updating the velocity model by a local optimization method. Thus, the new extended domain FWI approach automatically switches from a time-shift problem responsible for overcoming cycle-skipping, to a conventional least-squares FWI term for retrieving a high-resolution velocity model.

We firstly describe our new extended-domain FWI objective function and then discuss its convexity properties with respect to the time shifts. Finally, we demonstrate the effectiveness of the new FWI algorithm using synthetic and field data sets starting from simple initial models.

FWI objective function using time-warping extension

We start by introducing the time-warping extension $T(t)$ as a function of time so that the synthetic $u(t)$ and warped field data $d(T(t))$ are matched regardless of the initial model, i.e., $u(t) = d(T(t))$. The time-warping extension $T(t)$ is non-negative and satisfies the conditions $T(0) = 0$ and $T(t_{max}) = t_{max}$. As the velocity gets close to its target value, the time warping extension $T(t)$ approaches the actual physical time t, i.e., $T(t) = t$ so that the warped data $d(T(t))$ becomes the actual field data $d(t)$.

We formulate our new FWI objective function as:

$$J[m, T] = \frac{1}{2}||F[m] - d(T(t))||_2^2 + \frac{\lambda}{2}||t - T(t)||_2^2, \tag{1}$$

where m is the velocity model, $u = F[m]$ is the modeled data, λ is a positive trade-off parameter, $T(t)$ is the time-warping extension that dynamically transports the field data d towards the modeled data u and the difference $\tau(t) = t - T(t)$ is defined as the shift field which captures the relative time shifts between the modeled and field data.

We apply ADM to the optimization problem described in equation 1. First, the inner problem is solved by minimizing $J[m, T]$ over T for the time-warping extension using dynamic programming (e.g., Sakoe and Chiba, 1978). The resulting augmented cost function is:

$$T[m] = \underset{T}{\mathrm{argmin}} \frac{1}{2}||F[m] - d(T(t))||_2^2 \; + \frac{\lambda}{2}||t - T(t)||_2^2. \tag{2}$$

Additional constraints on the time-warping function can be applied in both time and spatial axes to enhance the lateral coherence (e.g., Ma and Hale, 2013). The outer problem is the minimization of the reduced objective function:

$$J_{red}[m] = \frac{1}{2}||F[m] - d(T[m])||_2^2 \; + \frac{\lambda}{2}||t - T[m]||_2^2. \tag{3}$$

Figure 1 shows the behavior of the reduced objective function (equation 3) with time-warping extension for large, medium and small values of λ compared with a least-squares FWI. The misfit function is computed by shifting a Ricker wavelet with central frequency of 8 Hz. As λ decreases, the reduced objective function moves from a least-squares objective function to the quadratic objective function which is related to the time shift and is responsible for tomographic updates.
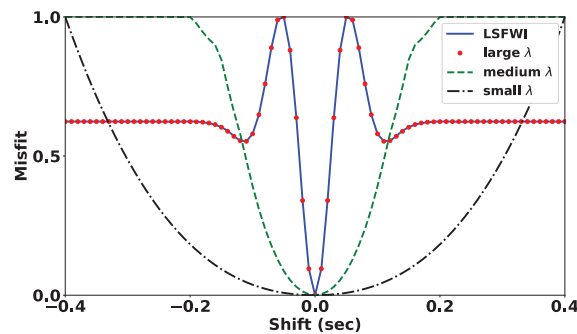

Figure 1 *Normalized misfit as a function of time shift for the least-squares (solid blue) and the reduced FWI objective functions with time-warping extension for large (dotted red), medium (dashed green) and small (dash-dotted black) values of λ. Note the least-squares FWI objective function completely coincides with the reduced FWI objective function for a large value of λ.*

Synthetic example

We use a modified version of the SEG-EAGE Overthrust model with a 1600 m water layer that simulates a marine setting (Figure 2a) to demonstrate the effectiveness of our approach. The input data were computed from this model using a filtered spike with corner frequencies of 3-5-10-13 Hz. The source/receiver deployment correspond to a fix-spread geometry. The initial model (Figure 2b) consists of a linearly increasing velocity with depth starting from the water bottom. This simple model produces a seismic response that comprises the waterbottom reflection and diving-wave energy which arrives later than the refracted events observed at far offsets in the input data (Figure 2e). For comparison, we perform both a conventional least-squares FWI and our FWI with time-warping extension without separation of reflections and refractions. The inverted model using the least-squares FWI (Figure 2c) is trapped in a local minimum and cannot reconstruct the central complex fault structures. In contrast, the inverted model, using the new approach (Figure 2d), accurately recovers all the features of the true model. This is validated by comparing a sample synthetic shot gather computed from the inverted models using a conventional (Figure 2f) and the new approach (Figure 2g) with the input data.

Field data example

We apply our FWI with time-warping extension to field data acquired in the Kwanza shelf area, offshore Angola. The acquisition comprises 12 multisensor streamers spaced 112.5 m apart, with a maximum inline offset of 8025 m. The maximum full-power frequency used in the inversion is 10 Hz. We performed the inversion from the initial model shown in Figure 3a using conventional least-squares FWI (Figure 3b) and the new extended domain FWI approach (Figure 3c). We show comparisons of the field and synthetic data at different offsets in Figures 3d-3f for a sample shot. The inversion is

performed using field data with minimum processing to remove the acquisition noise and without data selection. Notice that for the initial model, the simulated first arrivals are faster than those corresponding to the recorded refracted energy starting from the intermediate offsets, where there is cycle-skipping. Conventional least-squares FWI is not able to correct for this and provides even faster velocities (Figure 3b) in the shallow sediments. This increases the mismatch between field and modeled data at near and intermediate offsets. In contrast, the model after FWI using the new objective function (Figure 3c), shows the velocity reduction in the shallow part of the model and a clear definition of the high contrasted velocity zones corresponding to different carbonate formations (e.g., Katzaros et al., 2020). Figure 3f shows the validation of the new solution by comparing the field data with the simulated data using the inverted model. Note a good match of refracted and reflected energy along all the offsets.
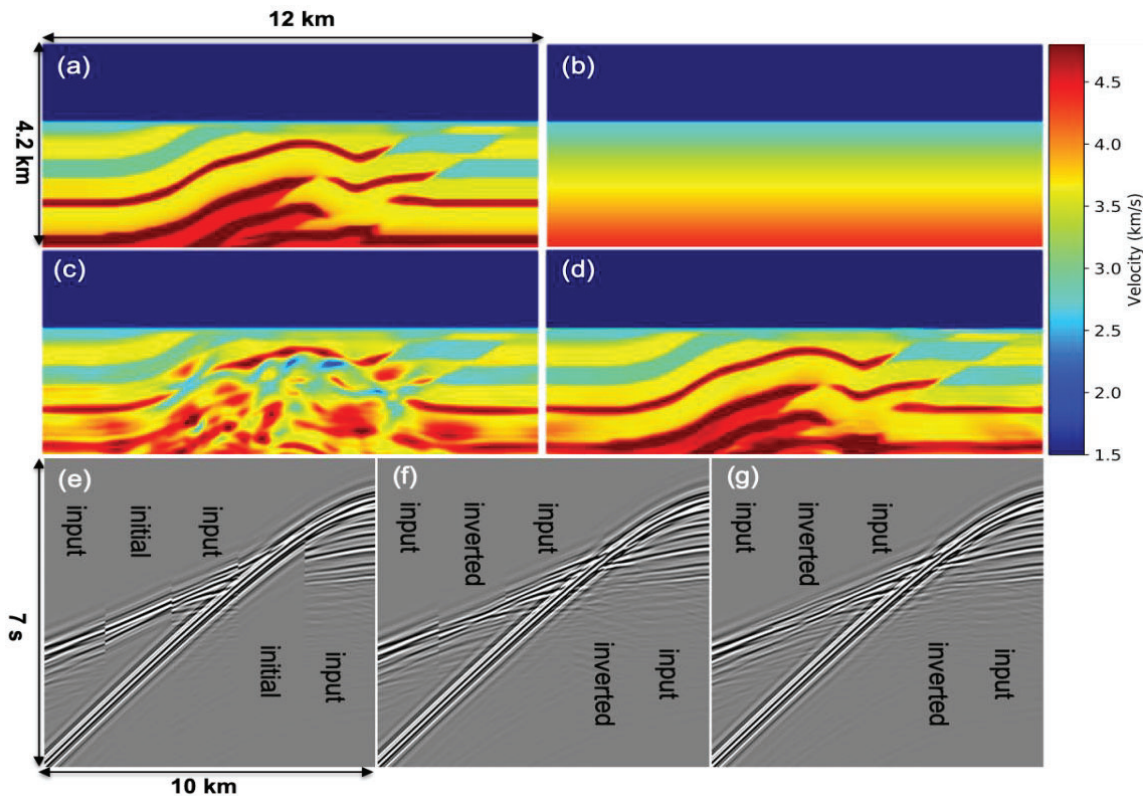

Figure 2 *Overthrust synthetic example. (a) True model; (b) 1D initial model; inverted models using (c) conventional least-squares FWI and (d) the new FWI approach. Comparison of input and synthetic data computed from (e) the starting model and the inverted models using the (f) conventional least-squares FWI and (g) the new FWI approach.*

Conclusions

We introduced a novel FWI objective function with time-warping extension to overcome cycle-skipping. The time-warping extension results in an objective function enabling automatic transition from a time-shift problem for overcoming cycle-skipping, to conventional least-squares FWI for improving the resolution of the velocity field. The new algorithm reduces the dependence on accurate initial models and/or the acquisition of low-frequency data. We successfully applied the new approach to a field data set demonstrating the retrieval of high-resolution velocity models starting from simple initial models with minimum data processing, which may reduce the turnaround time for building high-resolution velocity models.
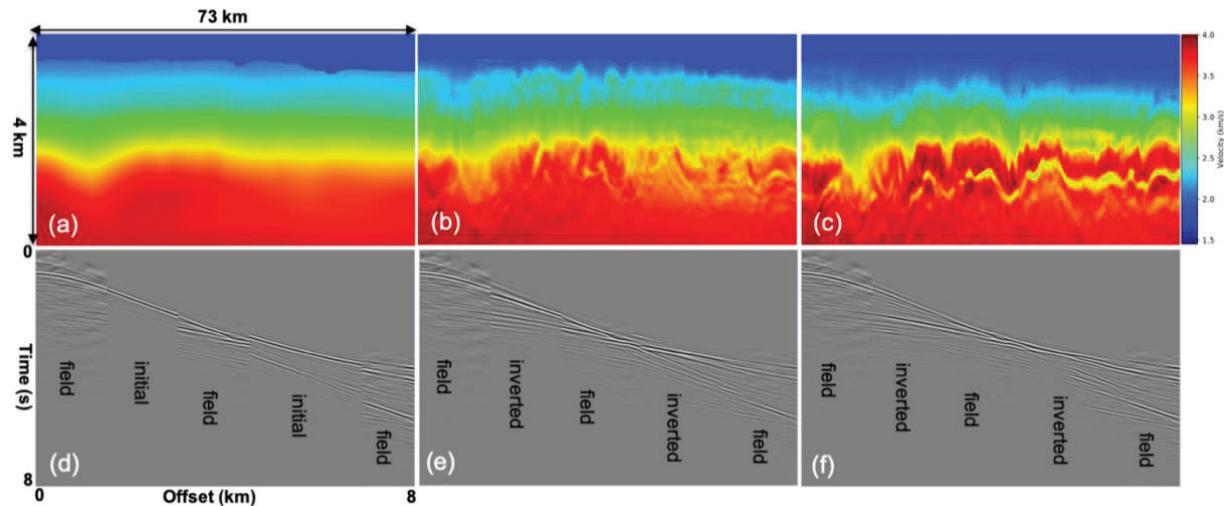
Acknowledgements

Figure 3 *Field data example. (a) Initial model and inverted model by (b) the least-squares FWI and (c) our FWI approach. Offset panel comparing the field data and the synthetic data using (d) the starting model and the inverted model by (e) the least-squares FWI and (f) our FWI approach.*

References

Biondi, B. and Almomin, A. [2013] Tomographic full-waveform inversion (TFWI) by combining FWI and wave-equation migration velocity analysis. *The Leading Edge*, **32**(9), 1074-1080.
Hale, D. [2013] Dynamic warping of seismic images. *Geophysics*, **78**(2), S105-S115.
Huang, G., Nammour, R. and Symes, W. W. [2017] Full-waveform inversion via source-receiver extension. *Geophysics*, **82**(3) R153-R171.
Luo, Y. and Schuster, G.T. [1991] Wave-equation traveltime inversion. *Geophysics*, **56**(5), 645-653.
Katzaros, G., Burrell, A., Colsoul, J. A. and Cahumba Quengue, N. R. [2020] Unlocking Hydrocarbon Prospectivity on the Angola Kwanza Shelf. *Geoexpro*, **17**(5), 23-24.
Ma, Y. and Hale, D. [2013] Wave-equation reflection travel-time inversion with dynamic warping and full-waveform inversion. *Geophysics*, **78**(6), R223-R233.
Métivier, L. and Brossier, R. [2020] A receiver-extension approach to robust full waveform inversion. *90th Annual International Meeting, SEG, Expanded Abstracts*, 641-645.
Sakoe, H., and S. Chiba [1978] Dynamic programming algorithm optimization for spoken word recognition. *IEEE Transactions on Acoustics, Speech, and Signal Processing*, **26**, 43–49.
Symes, W. W. [2008] Migration velocity analysis and waveform inversion. *Geophysical prospecting*, **56**(6), 765-790.
Tarantola, A. [1984] Inversion of seismic reflection data in the acoustic approximation. *Geophysics*, **49**,1259-1266.
Virieux, J. and Operto, S. [2009] An overview of full-waveform inversion in exploration geophysics. *Geophysics*, **74**(6), WCC1-WCC26.
Wang, M., Xie, Y., Xu, W.Q., Loh, F.C., Xin, K., Chuah, B.L., Manning, T. and Wolfarth, S. [2016] Dynamic-warping full-waveform inversion to overcome cycle skipping. *86th Annual International Meeting, SEG, Expanded Abstracts*, 1273-1277.
Yao, G., da Silva, N., Warner, M., Wu, D. and Yang, C. [2019] Tackling cycle skipping in full-waveform inversion with intermediate data. *Geophysics*, **84**(3), R411-R427.